Analysis of Parallel Photovoltaic Inverters with Improved Droop Control Method

Ruixing Lin
Sichuan Electric Power Research Institute
Chengdu 610072, China

Mao Yang
Sichuan Electric Power Research Institute
Chengdu 610072, China

Hongping Li*
School of Electrical Engineering and Information
Sichuan University
Chengdu 610065, China
* Corresponding author

***Abstract*—In this paper, an improved droop control strategy is presented to restrict the maximum power of inverters and to enhance the accuracy of reactive power sharing for parallel inverters in low voltage microgrid. The improved method can decouple active and reactive power through rotating orthogonal transformation, and extend traditional droop control to low voltage microgrid. The presented sine virtual active power-frequency droop control can restrict the maximum power of inverters without adding droop controlling unit of amplitude limits, and can enhance the accuracy of reactive power sharing. A microgrid simulation model is built in Matlab/Simulink simulation platform, and simulation analyses verify the validity and feasibility of the proposed strategy.**

Keywords-microgrid; parallel inverters; improved droop control; power sharing; maximum power

I. INTRODUCTION

Microgrids can be defined as a cluster of elements such as energy storage devices, energy conversion devices, protection devices, loads and distributed generations (DGs). With the increased concerns on environment and energy consumption, microgrids have recently received a great deal of attention [1]-[2]. Compared to DG units directly connect to grid, microgrids have less impact to the grid [3]. Distributed generations, such as photovoltaics, wind powers and fuel cell power generations, are connected to the grid via power electronic converters. A microgrid allows the DG units work in stand-alone mode and grid-connected mode [4]-[5]. When microgrid work in stand-alone mode, distributed generation mainly adopts droop control to make voltage stable and frequency within limits based on local information. Because droop control strategy does not depend on communication links and have “plug and play” feature, it has been widely used [6].

Because the line impedance ratio of low voltage microgrid is large, the traditional droop control has active power and reactive power coupling problems. To solve such problems, research members domestic and abroad had improved traditional droop control. In [7], an inverse droop control strategy when local line impedance ratio is high was proposed. In [8]-[9], in order to solve the problem which traditional droop control cannot be extended to low voltage microgrid with high impedance, presented *P-V, Q-ω* control strategy. It can achieve the purpose of active power and reactive power decoupling. But this method conflict with traditional generator droop characteristic, when DG connect to grid will make the system unstable, and influenced the stability of microgrid system.

To limit maximum output power of inverter, in [10], proposed joining power limitation control based on the droop control. In order to limit the voltage and frequency boundary value, literature [11] set the inverter maximum droop coefficient.

In order to share the load demand properly among inverters, literature [12] proposed a control strategy to mitigate errors in reactive power sharing by means of adjusting the droop coefficient of inverters. But excessive droop coefficient will cause the inverter output voltage and the point of common coupling (PCC) voltage drop.

In this paper, an improved droop control strategy is proposed for parallel operation inverters in low-voltage microgrid. To make the droop control can be used for a big impedance ratio of low voltage mcrogrid, control the output power using coordinate rotation transform, and realize a completely decoupled relationship between active power and reactive power. Then the improved sine virtual active power-frequency droop control is used. The method makes droop coefficient large near the rated power, and can make each DG unit share the total load in proportion to its rating. Further-more, the DG units can control the maximum output power under large load without maximum power limits link, and make the control of active power and frequency within limits.

© 2015. The authors - Published by Atlantis Press

II. MICROGRID STRUCTURE AND TRADITIONAL DROOP CONTROL

A. Microgrid Structure

Equivalent structure diagram of distributed generation in microgrid is shown in Figure 1. DG units can work in stand-alone mode and grid-connected mode.

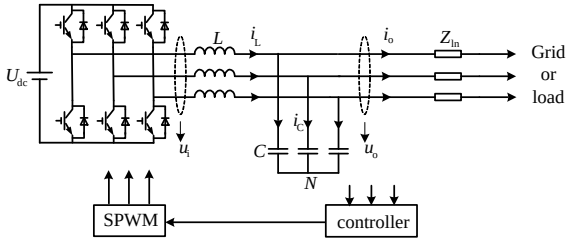

FIGURE I. STRUCTURE DIAGRAM OF THE MICROSOURSE

where U_{dc} is the equivalent of DC source, L is filter inductance, C is filter capacitor, Z_{ln} is the line impedance, i_L is circuit inductance current, i_C is capacitance current, i_o is output current of DG unit, u_i and u_o are inverter output voltage and capacitor voltage. Controller including voltage control loop and current control loop, realize voltage, frequency and power control. Inverters adopt the SPWM modulation method.

B. Traditional Droop Control

Figure 2 as the diagram for power flow of transmission line of a microsourse. The DG units are equivalent to the controlled voltage source, conveying power to the grid through the connection lines.

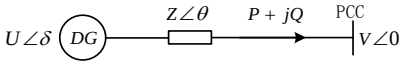

FIGURE II. POWER FLOW OF TRANSMISSION LINE OF A MICROSOURSE

where V is the voltage amplitude at PCC, U is voltage amplitude of DG unit, $Z=R+jX$ is comprehensive line impedance from DG to PCC, θ is comprehensive circuit impedance angle, P and Q is active and reactive power injected to line, δ is output voltage phase angle of DG unit.

From figure 2, the active power and reactive power inject into the bus by every inverter can be expressed as:

$$\begin{cases} P = \dfrac{U}{R^2 + X^2}[R(U - V\cos\delta) + XV\sin\delta] \\ Q = \dfrac{U}{R^2 + X^2}[X(U - V\cos\delta) - RV\sin\delta] \end{cases} \tag{1}$$

The expressions (1) can be simplified as:

$$\begin{cases} V\sin\delta = \dfrac{PX - QR}{U} \\ U - V\cos\delta = \dfrac{PR + QX}{U} \end{cases} \tag{2}$$

The line impedance is presented to be inductance in high voltage transmission line, that is X>>R, so resistance can be ignored in the control. Phase angle mainly depends on the active power, and voltage amplitude difference mainly depends on the reactive power.

Traditional droop control strategy simulates the synchronous generator interface operation features in high voltage grid, achieving the control for DG voltage, frequency and power. The control equations can be expressed as:

$$\begin{cases} \omega_i = \omega_0 - m_i P_i \\ U_i = U_0 - n_i Q_i \end{cases} \tag{3}$$

where ω_0 and U_0 are frequency and voltage amplitude references, P_i and Q_i are active and reactive power measured at output of DG unit, m_i and n_i are frequency droop coefficient and voltage droop coefficient, ω_i and U_i are frequency and voltage measured at output of DG unit.

Traditional droop control block diagram as shown in Figure 3.

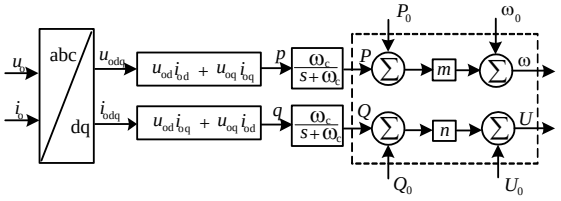

FIGURE III. BLOCK DIAGRAM OF TRADITIONAL DROOP CONTROL

The instantaneous output voltage and current of DG is transformed to dq0 coordinate. Then the instantaneous active power p and instantaneous reactive q are calculated. Performance of the control of the instantaneous power is not so well. Controling the average power is used to make the adjustment process relatively stable. Average active power P and reactive power Q are got through low-pass filter. Then reference frequency and voltage of DG units are obtained through droop control, which can be the input of voltage and current control loop.

III. IMPROVED CONTROL STRATEGY

A. Power Decoupling Based on Coordinate Transformation

In low voltage microgrid, the active and reactive power coupled, traditional droop control will no longer apply. Low voltage microgrid can't ignore the resistance and inductance circuit impedance any more, and frequency and voltage amplitude are no longer with the active and reactive power of one to one correspondence. Considering introducing rotating orthogonal coordinate transformation matrix T, the active and reactive power can be converted to the virtual active power and virtual reactive power through the coordinate transformation [10]. **T** for rotating coordinates orthogonal transformation matrix can be expressed as:

$$\mathbf{T}=\begin{bmatrix} \dfrac{X}{Z} & -\dfrac{R}{Z} \\ \dfrac{R}{Z} & \dfrac{X}{Z} \end{bmatrix}=\begin{bmatrix} \sin\theta & -\cos\theta \\ \cos\theta & \sin\theta \end{bmatrix} \tag{4}$$

In combination with formula (1), it can be converted to formula (5)

$$\begin{bmatrix} P' \\ Q' \end{bmatrix}=\mathbf{T}\begin{bmatrix} P \\ Q \end{bmatrix} \tag{5}$$

In combination with (2), (4), (5), in the case of low voltage microgrid, the expression of power flow can be expressed as:

$$\begin{cases} \delta \approx \dfrac{ZP'}{UV} \\ U-V=\dfrac{ZQ'}{U} \end{cases} \tag{6}$$

From type (6), it can be seen the traditional droop control is applied to low voltage microgrid. Phase angle δ and virtual active power P', voltage amplitude difference value $U–V$ and virtual reactive power Q' are one to one correspondence relation. We can create virtual active power-frequency and the reactive power voltage droop control, to control frequency, voltage and power in low voltage microgrid.

B. Improved Sine Virtual Active Power - Frequency Droop Control

In order to control the inverter output voltage and frequency within the scope of the permit, usually set a maximum coefficient or join prolapse limiter control links. If droop coefficient is too small, it will have big power sharing errors. Joining the limiter control links can make the control become more complex. This paper uses the sine droop control, making the droop coefficient changes with the power in a half cycle drab sine regular without adding limiter control links. This control strategy can adjust the droop coefficient automatically according to the inverter output power. When output power is not the same, the droop gain is also different. Near the rated power, droop coefficient is large, ensuring reactive power proportional sharing between the inverters. When output power of DG units are far away from rated power, that is when the output frequency is close to its limit, and droop coefficient will be adjusted to small, making frequency and power controlled in a limit area. Virtual reactive power and voltage not like phase is a one-to-one relationship with the active power, so voltage dose not use sinusoidal droop control. Sine virtual active - frequency droop control expressed as:

$$\omega=\omega_0-k\sin(l(P'-P_0')) \tag{7}$$

$$-\frac{\pi}{2}<l\Delta P'_{\max}<\frac{\pi}{2} \tag{8}$$

where k is sine droop control boundary value coefficient, l is sine droop control coefficient, l values by type (8) to determine, and $\Delta P'= P'- P_0'$. For different $\Delta P'$, l is different, that is it follows the change of the $\Delta P'$. For different capacity of DG units, the control has the versatility. Selecting suitable sine droop coefficient l make sine function input between $-\pi/2\sim\pi/2$, the selected sine function is easy to realize.

The block diagram of improved sine active power-frequency droop control is shown in Figure 4.

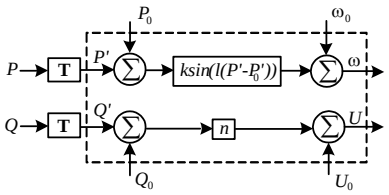

FIGURE IV. BLOCK DIAGRAM OF SINE DROOP CONTROL

Average power is obtained by traditional control method, virtual active and reactive power are got after a rotating orthogonal coordinate transformation matrix. Virtual active power controlled with the improved sine virtual droop control, and virtual reactive power using traditional droop control. Finally, we can get voltage and frequency reference value of the DG units.

Figure 5 as the diagram for the coefficient k and l impact to droop characteristics. Figure 5 illustrates the control coefficient k is mainly influence the frequency of the sinusoidal droop control boundary value, and control the range of frequencies for $(f–k/4)\sim(f+k/4)$Hz. Coefficient l mainly impact droop curve slope, and the larger l, the droop coefficient change more quickly.

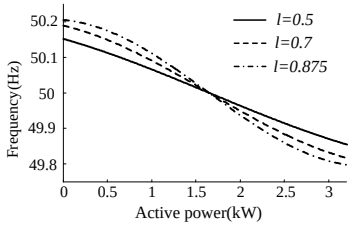

(a)

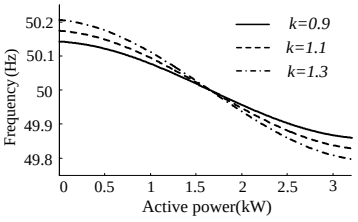

(b)

FIGURE V. THE EFFECT OF VARIATIONS IN SINE DROOP COEFFICIENTS. (A) VARIATIONS IN L. (B) VARIATIONS IN K.

Figure 6 as the traditional droop control and sine droop control characteristic curve. The Figure 6 shows that sine droop control characteristic curve is a smooth curve. Near the rated power, droop coefficient is large. When power changes, frequency adjusts to around frequency boundary, sine droop

control can provide relatively smooth curve asymptote. It can control the frequency and power not beyond the border without secondary regulation.

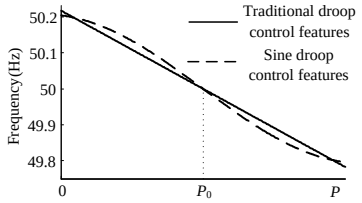

FIGURE VI. FREQUENCY DROOP CHARACTERISTICS

IV. SIMULATION RESULTS

To test and verify the validity and feasibility of the proposed sine droop control method. Simulation model of two parallel operation DG units is set up in Matlab/Simulink platform, which as shown in Figure 7.

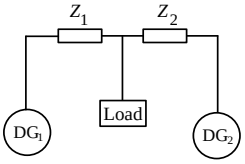

FIGURE VII. SIMULATION SYSTEM OF TWO PARALLEL DG UNITS

The simulation model contains two parallel operation photovoltaic inverters, supplying for the load. Frequency of the system is 50Hz, and voltage is 311V. DG resistance of transmission lines is presented to be inductance. DG_1 has the twice rated capacity of DG_2.Simulation control parameters and circuit parameters as shown in table **1**.

TABLE I. PARAMETERS OF THE SIMULATION

DG_1		**DG_2**	
Parameter	**Value**	**Parameter**	**Value**
DC voltage	800 V	DC voltage	800 V
Filter inductance	7mH	Filter inductance	7mH
Filter capacitor	25μF	Filter capacitor	25μF
Droop coefficient *k*	0.8	Droop coefficient *k*	0.8
Coefficient *l*	3	Coefficient *l*	3
Droop coefficient n	0.4V/kvar	Droop coefficient n	0.8V/kvar
Line impedance	0.2+j0.02 6Ω	Line impedance	0.17+j0.022 Ω

A. Calculation Case 1

Two DG units work in parallel operation. Before 0.6s, active and reactive power respectively 5kW, 2kvar. At 0.6s, load increases, and load active and reactive power is 6.5kW and 2.5kvar. Load active and reactive power increases to 8kW and 3var at 1.2s. DG units adopt traditional droop control and improved sine droop control, and output waveform of DG units is shown in figure 8.

From the Figure 8 (a), (d), it can be seen when the load changes, DG units with the improved droop control is quicker than the traditional droop control to achieve stable operation state. At 0.6s, load changes, and the traditional control from transient to steady state operation needs 0.12s, only 0.1s with the improve control. The figure 8(b), (e) show that the DG units which adopt the traditional droop control in different connection line impedance, can't share reactive power proportional. DG_1 with larger line impedance, shared reactive power is less than twice of the DG_2. However, the improved sine droop control strategy makes DG units sharing total reactive power in proportion to its rating. Near the rated power, the droop gain is large, and the transient process is short, also the distribution of reactive power deviation is reduced greatly. The figure 8(c) shows DG units adopt the improved droop control, when load power changes, system frequency change is small, within its limits.

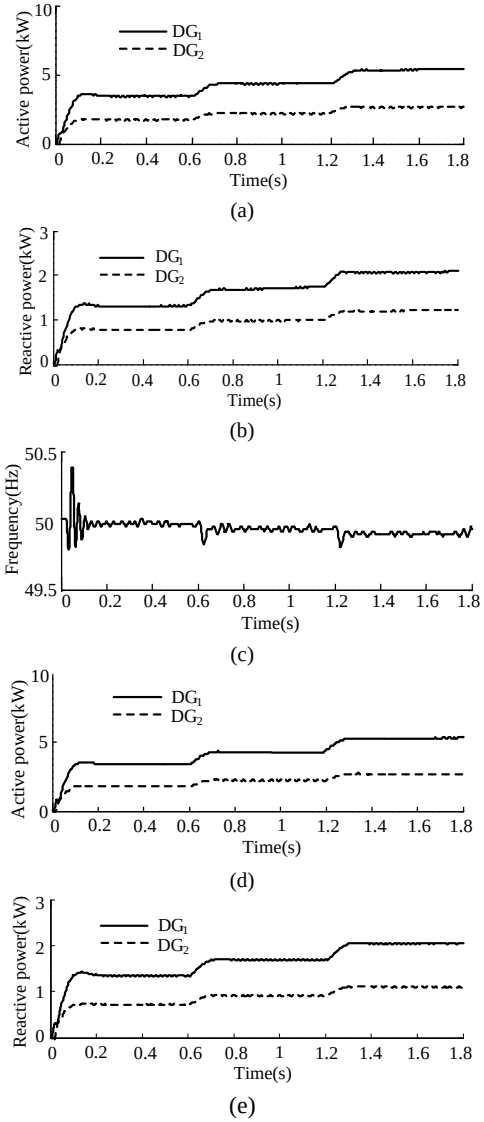

FIGURE VIII. SIMULATED RESULTS OF CASE 1. (A) ACTIVE POWER WITH TRADITIONAL DROOP CONTROL. (B) REACTIVE POWER WITH TRADITIONAL DROOP CONTROL. (C) FREQUENCY WITH SINE DROOP CONTROL. (D) ACTIVE POWER WITH SINE DROOP CONTROL. (E) REACTIVE POWER WITH SINE DROOP CONTROL.

B. Calculation Case 2

To test and verify improved control has the ability in limiting maximum output power, the simulation analyzes two

parallel operation DG units which supply for large load. Before 0.6s, active power is 5.25kW. Load active power increase to 12kW at 0.6s. DG units with the improved sine droop control, simulation waveform as shown in Figure 9.

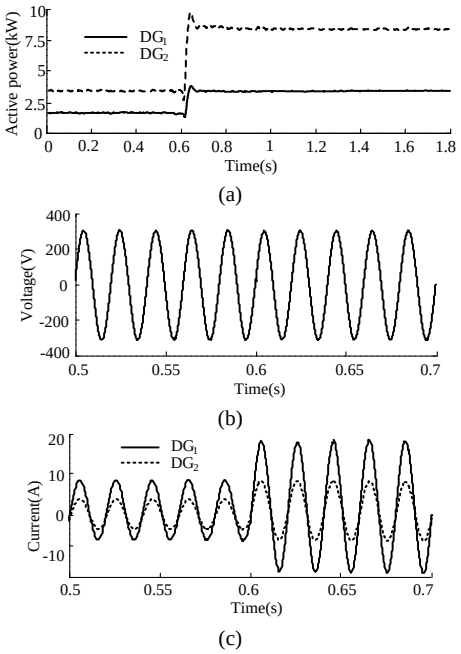

FIGURE IX. SIMULATED RESULTS OF CASE 2. (A) DG UNITS OUTPUT ACTIVE POWER. (B) VOLTAGE AT THE PCC. (C) DG UNITS OUTPUT CURRENT.

It can be seen from figure 9(a), that when the load power changes, DG_2 have maximum power output. Before 0.6s, DG_1 and DG_2 output active power are respectively 3.5kW, 1.75kW, and DG_1 shares the load power of 2 times the DG_2. After 0.6s, DG_1 and DG_2 output active power are 8.5kW and 3.5kW. Because the DG_2 has been restricted to maximum output power at 0.6s, so other power is borne by the DG_1, and DG_1 output capacity is greater than 2 times of DG_2. Droop coefficient of sine droop control change with the output power. When close to the maximum output power boundaries, droop coefficient will decrease, and finally asymptote way towards zero and the output power will be restricted to a maximum value. From the figure 9(b), (c), it can be seen that power changes and the PCC point voltage remains the same, and DG units output current changes with output power.

V. CONCLUSION

The method presented in this paper is based on traditional droop control method, adding rotary coordinate transformation and sine virtual active power-frequency droop control strategy. Droop coefficient of this method is large near the DG rated power, and has accurate frequency control, and power sharing is in proportional. In deviating from the DG rated power, sine droop coefficient will be small, and finally tends to zero. Thus, the method does not need to set the maximum droop coefficient and the secondary power limit links can be able to limit the maximum output power of the DG units. Sine virtual active power-frequency droop control is simple and feasible. The simulation results verify the correctness and feasibility of the proposed control strategy.

REFERENCES

[1] Ding Ming, Zhang Yingyuan, Mao Meiqin. Key technologies for microgrids being researched[J]. Power System Technology, 2009, 33(11) : 6-11.

[2] Wang Shaoyong. Design and operation of microgrid based on distributed generation[J]. Electric Power Automation Equipment, 2011, 31(4) : 120-123.

[3] Wang Chengshan, Xiao Zhaoxia, Wang Shouxiang. Synthetic control and analysis of microgri[J]. Automation of Electric Power Systems, 2008, 32(7) : 98-103.

[4] Zhao Dongmei, Zhang Nan, Liu Yanhua, et al. Synthetical control strategy for smooth switching between grid-connected and islanded operation modes of microgrid based on energy storage system[J]. Power System Technology, 2013, 37(2) : 301-306.

[5] Zhang Ying, Wu Chunsheng, Wang Yibo, et al. Study on smooth transition in micro-grid system[J]. Renewable Energy Resources, 2013, 31(8) : 14-17.

[6] Zhang Yao, Ma Hao, Lei Biao, et al. Analysis of dynamic performance for parallel operation wire interconnections[J]. Proceedings of the CSEE, 2009, 29(3) : 42-48.

[7] De Brabandere K, Bolsens B, Van Den Keybus J, et al. A Voltage and Frequency Droop Control Method for Parallel Inverters[J]. IEEE Transactions on Power Electronics, 2007, 22(4) : 1107-1115.

[8] Rocabert J, Luna A, Blaabjerg F, et al. Control of power converters in AC microgrids[C]. IEEE Transactions on Power Electronics, 2012, 27(11) : 4734–4749.

[9] Sun Xiaofeng, Lü Qingqiu. Improved PV Control of Grid-Connected Inverter in Low Voltage Micro-Grid[J]. Transactions of China Electrotechnich Society, 2012, 27(11): 4734–4749.

[10] Zhou Xianzheng, Rong Fei, Lü Zhipeng, et al. A coordinate rotational transformation based virtual power V/f droop control method for low voltage microgrid[J]. Automation of Electric Power Systems, 2012, 36(2) : 47-52.

[11] Aghasafari M A, Lopes L A C, Williamson S. Frequency Regulation and Enhanced Power Sharing in Microgrids Including Modified Droop Coefficients and Virtual Resistances[J]. IEEE Electrical Power & Energy Conference, Montreal, Canada, 2009.

[12] Majumder R, Chaudhuri B, Ghosh a, et al. Improvement of stability and load sharing in an autonomous microgrid using supplementary droop control loop[J]. IEEE Transactions on Power Electronics, 2010, 25(2) : 796-808.